

SEIR Model-Based Evaluation of the impact of Smoking Recruitment rates on Lung Cancer Incidence and Prevalence

^{*1}Nwagor, P., & ²Oghenrhoro, P. S.

¹Department of Mathematics, Ignatius Ajuru University of Education, Port Harcourt, Nigeria.

²Department of Environmental Management and Toxicology, Dannis Osadebay University, Asaba, Nigeria

***Corresponding author email:** peter.nwagor@iaue.edu.ng

Abstract

Lung cancer is one of the leading causes of cancer-related deaths worldwide, with tobacco smoking being the primary risk factor. This study develops an SEIR (Susceptible-Exposed-Infected-Removed) model to investigate the impact of smoking recruitment rates on lung cancer incidence and prevalence. The systems of non-linear ordinary differential equations were used to define the dynamics of Lung cancer, which involves the recruitment rate. The analysis of a total population size in a region $N(t)$ at any time t which is subdivided into five compartments such as, $S(t)$ (susceptible population that is the vulnerable subpopulation who are not infected with lung cancer, but at a high risk of infection as a result of smoking), population who are active smoker $E_a(t)$, population who are victim of smoking $E_p(t)$, number of individual infected with lung cancer $I(t)$ and number of population recovered from lung cancer $R(t)$ was involved in the study. The positivity, uniqueness and boundedness of solutions were verified, whereas the sensitivity and basic reproductive number were determined analytically. Numerical simulations are performed to explore the effects of varying smoking recruitment rates on lung cancer burden. The results show that reducing smoking recruitment rates can significantly decrease lung cancer incidence and prevalence. Results show that the number of lung cancer cases originating from the active smoker population and higher values of recruitment rate led to increased lung cancer cases among smokers. Increased active smoker recruitment rate (a) leads to higher smoking prevalence, increased lung cancer incidence, and higher mortality rates. Also increased rate of population becoming victim of smoking (b) leads to higher smoking prevalence, increased lung cancer incidence and higher mortality rates. The study recommends implementing advocacy on the Reduction of smoking recruitment rates through education campaigns and promotion of an increase in lung cancer screening and early detection with sound policies to reduce lung cancer incidence rates. The study suggests that enhancing antagonistic relationships between tumour-promoting and suppressive factors could improve the robustness of anti-cancer strategies, making tumours more controllable.

Keywords: SEIR Model, Intervention Strategy, Disease Mitigation, Cigarette Smoking, Lung Cancer

Introduction

Lung cancer is one of the leading causes of cancer-related deaths worldwide, accounting for approximately 2.1 million new cases and 1.8 million deaths annually. Tobacco smoking is the primary risk factor for lung cancer, responsible for about 80-90% of all lung cancer deaths (Ekeanyanwu et al., 2025). Smoking recruitment rates, which refer to the rate at which new individuals initiate smoking, play a crucial role in determining the incidence and prevalence of lung cancer.

Mathematical modelling has emerged as a valuable tool in understanding the dynamics of lung cancer and the impact of various factors, including smoking recruitment rates, on its incidence and prevalence. The SEIR (Susceptible-

Exposed-Infected-Removed) model, a compartmental model that divides the population into distinct groups based on their disease status, has been widely used to study the transmission dynamics of infectious diseases (Nwagor & Ekaka-a, 2017). However, its application to the study of lung cancer, a non-communicable disease, is relatively novel.

This study aims to develop an SEIR model that incorporates the impact of smoking recruitment rates on lung cancer incidence and prevalence. By exploring the dynamics of lung cancer in the context of smoking behavior, this model seeks to provide insights into the potential effects of smoking prevention and cessation strategies on lung cancer burden. The findings of this study can inform public health policy and interventions aimed at reducing the incidence and prevalence of lung cancer.

A lot of infectious diseases have been studied by experts in mathematical modelling and simulations. Biomathematics and epidemiology of chronic diseases (Nwagor, 2020). Lung cancer is the leading cause of cancer deaths worldwide, with approximately 2.09 million new diagnoses each year and around 1.76 million deaths. Lung cancer can start anywhere in the lungs and affect any part of the respiratory system. Unlike normal cells, cancer cells grow without control and destroy the healthy lung tissue around them. This growth can spread, or metastasise, beyond the lung to the lymph nodes by the process of metastasis into nearby tissue or other parts of the body.

Modelling of Lung Cancer Dynamics

Modelling the dynamics of the impact of smoking on the lungs can be done through various mathematical and computational approaches, including Ordinary Differential Equations (ODEs), Partial Differential Equations (PDEs), and Agent-Based Models (ABMs), which involve simulating the interactions between lung cells, inflammatory agents, and smoke particles. Network Models, which also involve the interactions between different lung regions and the spread of damage. Machine Learning (ML) and Artificial Intelligence (AI). These models can be informed by experimental data from in vitro and in vivo studies, as well as clinical data from smoking-related lung disease patients. SIRS Susceptible (S), Infected (I) recovery (R) and susceptible (S) model is an extension of the SIR (susceptible, Infected, recovered) model, where it is believed that individuals can become Coronavirus infections have been studied by many researchers and epidemiologists to curtail the disease and its further spread in the community. The researchers tried to develop the vaccine and vaccinated most of the individuals in order to better reduce the number of infected people and their future spread. Although with the passage of time and the emergence of the new variants of coronavirus, the world is still facing infections in many countries. Some mathematical models in integer and non-integer orders to study the viral infections are discussed in this paper. The optimal control analysis for the elimination or control of the disease in Pakistan, by considering the real coronavirus cases, has been studied in Trisilowati. (2019), infectious diseases is transferrable to other healthy humans very fast, so the best and most effective way is to reduce the infection, is the isolation and quarantine, which is discussed through a mathematical modelling approach by the authors in Ayinde (2020) and Nabi et al. (2020), Lockdown and its impact on disease control was also considered using an SEIR modelling approach while adopting real data from Italy and France and presented the disease control scenario for the epidemic. Different reported cases and their modelling in Nigeria, with comparison, have been discussed in (Nwagor & Ekaka-a, 2017). A fractional study on COVID-19 to address the isolation, quarantine, and environmental vital loads has been explored (Nwagor & Lawson-Jack, 2020). A robust study on COVID-19 in a fractional environment is considered in (Okeke et al., 2019; Zhang et al., 2020). The analysis of the COVID-19 infection modelling for the real cases in sub-Saharan Africa has been discussed in Okeke et al.(2017).

Cigarette Smoking and Lung Cancer Prevalence

Considering all the fatalities of lung cancer, a model-based study on lung cancer was discussed by many mathematicians. Several mathematical models have been proposed on smoking behaviour and lung cancer. Acevedo-Estefania et al. (2000) constructed the model to describe the dynamics of lung cancer at the population level caused by smoking and secondhand smoke. The model determined that the best way to lower the number of smokers and individuals developing lung cancer is by increasing the number of well-educated individuals about the effects of smoking.

Andest (2013) also formulated a mathematical model that describes nicotine accumulation in the lungs of a smoker, which is the main cause of lung cancer. Wardah et al. (2017) presented a mathematical model that discusses of lung cancer as the effect of smoking behaviour on both active and passive smokers. Trisilowati (2019) analyses the stability

as well as uses an optimal control strategy on Wardah et al. (2017) model and illustrates that the optimal control is effective in controlling the growth of passive, active smokers and lung cancer patients. There is an extensive body of work which develops models associated with the treatment of cancer using chemotherapy, radiotherapy, targeted agent treatment, etc. Beljanski and Hiscott (2012) mentioned that multidrug resistance to this treatment is the major cause of failure in clinical treatment.

Genetically modified oncolytic viruses (OVs) kill tumour cells via unique mechanisms compared to other treatments. Thus, Beljanski Hiscott. (2012) claims that treatments with oncolytic viruses (OVs), which are under development, will open the possibility to overcome drug resistance and modulate the immune response to fight against cancer.

Taking the above discussions into account, we propose a model to study the dynamics of lung cancer and its relation with cigarette smoking. Many theoretical as well as mathematical models of lung cancer have been proposed by researchers. But this is a newly proposed mathematical model of lung cancer on the basis of some basic assumptions. It is observed from real phenomena that patients recovered from lung cancer are not out of danger at all; they can be affected with lung cancer again. It indicates that people recovered from lung cancer are becoming susceptible again and can develop this fatal disease multiple times. It is in the interest of this study to examine the dynamics of lung cancer and the relation to cigarette smoking using a computational approach.

Fractional calculus is gaining attention from researchers around the world due to its many properties and its applications to physical and engineering problems. The heredity properties, the memory, and the crossover behaviour can only be observed in a model with a fractional-order system. The fractional calculus with different fractional operators and their applications have been found, in integro-differential equations (Wang, 2022), Karthikeyan et al (2021), the development in the operators (Umoh & Nwagor, 2024), application to epidemiology (Umoh & Nwagor, 2024b), application to wave dynamics equations..

Aim and Objectives of the Study

The goal is to define a suitable mathematical model for assessing lung cancer incidence and prevalence, focusing on specific objectives:

1. Study the biological dynamics of lung cancer transmission.
2. Calculate the basic reproduction number and determine smoke-free and endemic equilibrium points.
3. Evaluate the effect of smoking recruitment rate on lung cancer incidence and prevalence.

Mathematical Formulation

A mathematical model of a system of nonlinear ordinary differential equations (ODEs) will be studied in this study. The basic reproduction number will be determined by next generation matrix. The condition for the existence of equilibrium points (smoke-free and endemic equilibrium points) and their stability analysis will be investigated. Considering a total population size in a region is $N(t)$ at any time t which is subdivided into five compartments such as, $S(t)$ (susceptible population that is the vulnerable subpopulation who are not infected with lung cancer, but at a high risk of infection as a result of smoking), population who are active smoker $E_a(t)$, population who are victim of smoking $E_p(t)$, number of individual infected with lung cancer $I(t)$ and number of population recovered from lung cancer $R(t)$. Considering the above compartments, the mathematical model of the dynamics of Lung cancer can be represented by the following system of non-linear ordinary differential equations

$$\begin{aligned}\frac{dS}{dt} &= r - (a + b)E_a S - mS + hR \\ \frac{dE_a}{dt} &= aE_a S + eE_p - gE_a - mE_a \\ \frac{dE_p}{dt} &= bE_a S - eE_p - dE_p - mE_p \\ \frac{dI}{dt} &= gE_a + dE_p - SI - (m + f)I \\ \frac{dR}{dt} &= SI - (m + h)R\end{aligned}\tag{1}$$

In the above model, r is the natural growth rate of population, m is the natural mortality rate, a and b is the rate at which susceptible population become active and passive smoker respectively. We are not involving the interaction between the passive and active smoker population, and e is the rate of passive smokers transforming into active smokers. The constant g and d represent the rate at which active and passive smokers become infected with lung cancer.

The constant s represents the recovery rate from lung cancer by getting proper treatment and f represents the disease-induced death rate. In real life, despite getting treatment and recovering from lung cancer, people may become susceptible to lung cancer again, and the rate is denoted by h .

Model Analysis

The model (1) has to be analysed in order to describe the dynamics of lung cancer. This analysis desires to show the effect of smoking on lung cancer, and the objective of this analysis is to control the adverse situation in the locality.

Since it is impossible to find the exact solution of the nonlinear autonomous system (1), we have to analyse the qualitative behaviour of the solutions in the neighbourhood of the equilibrium points. First, we find the boundedness and positivity of the solutions, then find out the equilibrium points, followed by analysing the stability of the equilibrium points and basic reproduction number R_0 . The basic reproduction ratio is important because it tells us if a disease will persist or extinct. For the analysis of model (1), a closed set has been considered as

$$\Omega = \left\{ (S(t), E_a(t), E_p(t), I(t), R(t)) \in \mathbb{R}_+^5 \mid 0 \leq N \leq \frac{r}{\mu} \right\}$$

with initial condition $S(0) > 0, E_a(0) \geq 0, E_p(0) \geq 0, I(0) \geq 0, R(0) \geq 0$

Boundedness of Solutions of the Model

We have to show that the total population is bounded for all $t \geq 0$.

Lemma 1: The region $\Omega = \left\{ (S(t), E_a(t), E_p(t), I(t), R(t)) \in \mathbb{R}_+^5 \mid 0 \leq N \leq \frac{r}{\mu} \right\}$ is positively invariant set for the model (1)

Proof: Since the population size is $N(t)$ so that $N(t) = S(t) + E_a(t) + E_p(t) + I(t) + R(t)$

Now the rate of change of total population is $\frac{dN}{dt} = \frac{dS}{dt} + \frac{dE_a}{dt} + \frac{dE_p}{dt} + \frac{dI}{dt} + \frac{dR}{dt}$

$$\begin{aligned} \Rightarrow \frac{dN}{dt} &= r - \mu(S + E_a + E_p + I + R) - \phi I \\ &\Rightarrow \frac{dN}{dt} + \phi I = r - \mu N \end{aligned}$$

In the absence of the disease lung cancer (i.e. $I = 0$), we

get dN , $\frac{dN}{dt} \leq r - \mu N$.

Now Substituting this, we obtain

$$N(t) \leq \frac{r}{\mu} + \left(N_0 - \frac{r}{\mu}\right) e^{-\mu t}$$

It is clear from solving that the total population $N(t)$ will approach the threshold $\frac{r}{\mu}$ as $t \rightarrow \infty$

This indicates that if the initial total population N_0 is less than $\frac{r}{\mu}$ i.e. if $N_0 \leq \frac{r}{\mu}$ then $N(t) = \frac{r}{\mu}$. so, definitely $\frac{r}{\mu}$ is the upper bound of N

On the other hand, if $N_0 > \frac{r}{\mu}$, then $N(t)$ will decrease to $\frac{r}{\mu}$ as $t \rightarrow \infty$. This means that $N_0 > \frac{r}{\mu}$, then the solutions $(S(t), E_a(t), E_p(t), I(t), R(t))$ enters the region Ω or approaches it asymptotically

Thus, we conclude that the region Ω is positively invariant under the flow induced by the model (1). Therefore, the model is both mathematically and epidemiologically well-posed in the region Ω . It is therefore sufficient to study the dynamics of the model (1) in Ω . Hence the lemma is proved.

Positivity of solution of the Model

Since the model (1) describes the human population, it is necessary to prove that all the state variables $S(t), E_a(t), E_p(t), I(t), R(t)$ are non-negative i.e. the solutions of the model (1) with positive initial conditions, $S(0) > 0, E_a(0) \geq 0, E_p(0) \geq 0, I(0) \geq 0, R(0) \geq 0$, are non-negative " $t > 0$."

Lemma.2: If $S(0) > 0, E_a(0) \geq 0, E_p(0) \geq 0, I(0) \geq 0$, and $R(0) \geq 0$, then the solutions $S(t), E_a(t), E_p(t), I(t), R(t)$ of the model (1) are all non-negative for all $t \geq 0$.

Proof:

The initial conditions for the model (1) is, $S(0) \geq 0, E_a(0) \geq 0, E_p(0) \geq 0, I(0) \geq 0, R(0) \geq 0$. The first equation of the model (3.1) is denoting the rate of change of susceptible

$$\text{population with time. } \frac{dS}{dt} = r - (a + b)E_a S - mS + hR \quad (7)$$

For Positivity, (7) can be written as, $\frac{dS}{dt} + mS = r$ (8)

$$bS^3 \frac{r}{m} + ce^{-m} \quad (9)$$

Applying initial condition, (at $t = 0, S(0) \geq 0$), we get from (3.1 – 3.5), $c = S(0) - \frac{r}{m}$

By putting the value of C in (9) we get,

$$S(t)^3 \frac{r}{m} + \dots - \frac{r}{m} e^{-mt} \quad (10)$$

So, at $(r(R)\Psi, S(t)^3 \frac{r}{m})$, which is also greater than 0

So, the first solution $S(t)$ of the model (1) is positive for all $t \geq 0$,

Therefore, all the solutions $(S(t), E_a(t), E_p(t), I(t), R(t))$ of the dynamic model (1) with positive initial conditions $S(0) \geq 0, E_a(0) \geq 0, E_p(0) \geq 0, I(0) \geq 0, R(0) \geq 0$, are non-negative for all $t \geq 0$.

Smoke –Free Equilibrium Point

An equilibrium points of a system with no infections or diseases is called disease equilibrium point. Let us consider the smoke free equilibrium point of the model (1) W_0 . In case of smoke free equilibrium point for the model (1) all this state variables E_a, E_p, I, R are zero except the susceptible compartment S

So

$$\frac{dS}{dt} + \frac{dE_a}{dt} + \frac{dE_p}{dt} + \frac{dI}{dt} + \frac{dR}{dt} = 0$$

$$\text{Hence we get, } r - mS = 0$$

$$pS = \frac{r}{m}$$

So, the smoke free equilibrium for the model (1) is, $w_0 (S, E_a, E_p, I, R) = \left(\frac{r}{m}, 0, 0, 0, 0\right)$

Endemic Equilibrium Point

Let the endemic equilibrium point for the (1) model be $w_1(S^*, E_a^*, E_p^*, I^*, R^*)$

That can be obtained by considering

$$\frac{dS^*}{dt} = \frac{E_a^*}{dt} = \frac{E_p^*}{dt} = \frac{I}{dt} = \frac{R^*}{dt} = 0$$

This implies that

$$\frac{dS}{dt} = r - (a + b)E_a^*S^* - mS^* + hR^* = 0 \quad (11)$$

$$\frac{dE_a}{dt} = aE_a^*S^* + eE_p^* \cdot gE_a^* \cdot mE_a^* = 0 \quad (12)$$

$$\frac{dE_p}{dt} = bE_a^*S^* \cdot eE_p^* \cdot dE_p^* \cdot mE_p^* = 0 \quad (12)$$

$$\frac{dI}{dt} = gE_a^* + dE_p^* \cdot SI^* \cdot (m + f)I^* = 0 \quad (13)$$

$$\frac{dR}{dt} = sI^* \cdot (m + h)R^* = 0 \quad (14)$$

By solving the equation, (1) we get the endemic equilibrium point is $w_0^o(S^*, E_a^*, E_p^*, I^*, R^*)$ where,

$$\begin{aligned} S^* &= \frac{K_1 K_2}{\alpha K_1 + \varepsilon \beta} \\ E_a^* &= \left| \frac{K_1 K_2 K_4 (r - mS^*)}{K_1 K_3 K_4 K_5 S^* - hs(gK_1 + abS^*)} \right| \\ E_p^* &= \frac{\beta E_a^* S^*}{K_1} \\ I^* &= \frac{gK_1 + abS^*}{K_1 K_3} (E_a^*) \\ R^* &= \left| \frac{S(gK_1 + abS^*)}{K_1 K_3 K_4} \right| (E_a^*) \end{aligned}$$

Also $K_1 = \varepsilon + \delta + \mu$, $K_2 = \gamma + \mu$, $K_3 = \sigma + \mu + \phi$, $K_4 = \mu + \tau$, $K_5 = \alpha + \beta$

2.7 Basic Reproduction Number

The basic reproduction number is defined as the secondary infections produce by one primary infection in a holy susceptible population it is a key epidemiological quantity because it determines the size and duration of epidemics Here the F_i is the gains to infections compartments V_i is the losses from infections compartment

$$F_i = [F_1 \ F_2 \ F_3] = [\alpha E_a S \ \beta E_a S \ 0] \text{ and } [V_1 \ V_2 \ V_3] = [(\gamma + \mu)E_a - \varepsilon E_p \ (\varepsilon + \delta + \mu)E_p \ (\sigma + \mu + \phi)I - (\gamma E_a + \delta E_p)] \quad (15)$$

At the disease-free equilibrium point $F = \left(\frac{r}{\mu}, 0, 0, 0, 0\right)$

We have

$$F = \begin{bmatrix} \frac{\alpha r}{\mu} & 0 & 0 & \frac{\beta r}{\mu} & 0 & 0 & 0 & 0 \end{bmatrix} \quad (16)$$

$$V = [\gamma + \mu \ -\varepsilon \ 0 \ 0 \ \varepsilon + \delta + \mu \ 0 \ -\gamma \ -\delta \ \sigma + \mu + \phi] = [K_2 \ -\varepsilon \ 0 \ 0 \ K_1 \ 0 \ -\gamma \ -\delta \ K_3] \quad (17)$$

Where $\varepsilon + \delta + \mu = K_1$, $\gamma + \mu = K_2$ and $\sigma + \mu + \phi = K_3$

Now the characteristics equilibrium is given by setting $\det(G - \lambda I) = 0$, where $G = FV^{-1}$ Therefore

$$\begin{aligned}
G - \lambda I &= \begin{bmatrix} \frac{\alpha r}{\mu K_2} - \lambda & \frac{\alpha r \varepsilon}{\mu K_1 K_2} & 0 & \frac{\beta r}{\mu K_2} & \frac{\beta r \varepsilon}{\mu K_1 K_2} & -\lambda & 0 & 0 & 0 & -\lambda \end{bmatrix} = 0 \\
&\Rightarrow \left(\left(\frac{\beta r \varepsilon}{\mu K_1 K_2} - \lambda \right) \left(\frac{\alpha r}{\mu K_2} - \lambda \right) - \frac{\alpha \beta \varepsilon r^2}{\mu^2 K_1 K_2^2} \right) (-\lambda) = 0 \\
\lambda &= \frac{r(\alpha K_1 + \beta \varepsilon)}{\mu K_1 K_2}, \quad 0, \quad 0
\end{aligned} \tag{18}$$

Equating (18) follows that the basic reproduction number is given by the largest eigen value for the model (1) is

$$R_0 = \frac{r(\alpha K_1 + \beta \varepsilon)}{\mu K_1 K_2}$$

Stability at Smoke Free and endemic Equilibrium Point

Theorem 1: The smoke free equilibrium point is locally asymptotically stable if $R_0 < 1$ and unstable if $R_0 > 1$

Proof:

In order to perform the stability analysis at smoke free equilibrium point w_0 , we have the Jacobian matrix of the model (1) at smoke free equilibrium point $w_0 = (\frac{r}{m}, 0, 0, 0, 0)$

$$J(w_0) = \begin{vmatrix} m & 0 & 0 & 0 & 0 & -\frac{rk_3}{m} & \frac{ar}{m} & -k_2 & \frac{br}{m} & g & 0 & 0 & e & -k_1 & d & 0 & 0 & 0 & 0 & -k_3 & s & h & 0 & 0 & 0 & -k_4 \end{vmatrix}$$

Let I be the eigen value and I be the identity matrix, then the characteristic equation is,

$$\begin{aligned}
|J(w_0) - I| &= \begin{vmatrix} -m - I & 0 & 0 & 0 & 0 & -\frac{rk_3}{m} & \frac{ar}{m} & -k_2 - I & \frac{br}{m} & g & 0 & 0 & e & -k_1 - I & d & 0 & 0 & 0 & 0 & -k_3 - I & s & h & 0 & 0 & 0 & -k_4 - I \end{vmatrix} \\
&= 0
\end{aligned} \tag{19}$$

Solving this, implies that

$$(-M - I)(-k_3 - I)(-k_4 - I)(I^2 + a_1 I + a_2) = 0 \tag{20}$$

Where $a_1 = k_1 + k_2 - \frac{ar}{m}$

$$= k_1 + k_2(1 - R_0) + \frac{r\beta\varepsilon}{\mu k_1} \tag{21}$$

and

$$a_2 = k_1 k_2 - \frac{ark_1}{m} - \frac{ber}{m} = k_1 k_2(1 - R_0) \tag{22}$$

The eigen value $\lambda_1 = -\mu$, $\lambda_2 = -k_3 = -(\sigma + \mu + \phi)$ and $\lambda_3 = -k_4 = -(\mu + \eta)$ are the negative roots of the characteristic polynomial. The Routh-Hurwitz criterion is used to show that the remaining polynomial, $I^2 + a_1 I + a_2 = 0$ has negative real roots. According to the Routh-Hurwitz criteria of second order polynomials, the system is asymptotically stable if $a_1 > 0$ and $a_2 > 0$. Here a_1 as well as a_2 will be positive when $R_0 < 1$. Therefore, the smoke free equilibrium point $w_0 = (\frac{r}{m}, 0, 0, 0, 0)$ is locally asymptotically stable if $R_0 < 1$ and unstable if $R_0 > 1$. The stability of the endemic equilibrium point w_1 is analysed as to have the theorem (2) to determine the stability of the endemic equilibrium point w_1 .

Numerical Results

The numerical simulations of our model proposed in (1) was performed using the python solver. All the values of the parameters used in (1) are obtained from different organizations such as the CDC (Center for Disease Control), American Lung Cancer Society, WCRF (world cancer research foundation), WHO (world health organization) Global cancer observatory (GLOBOCAN) and other non-profit and government agencies. The calculated available data from these sources and approximate result have been taken which fits into the model more appropriately.

Table 1 Definitions and values of Parameters of the Model

Descriptions	Parameters	Values
growth rate of population	r	0.05 d^{-1}
natural mortality rate	m	0.01 d^{-1}
active smoker recruitment rate from susceptible population	a	0.25
rate of population become victim of smoking	b	0.75
rate of population migrate from victim group to smokers	e	0.35
smoker's lung cancer incidence rate	g	0.2
lung cancer incidence rate from victim group	d	0.05
lung cancer recovery rate	s	0.2
cancer incident mortality rate	f	0.6
migration rate from recovered to susceptible compartments	h	0.5

Presentation of Results

The impact of smoking recruitment rates on lung cancer incidence and prevalence

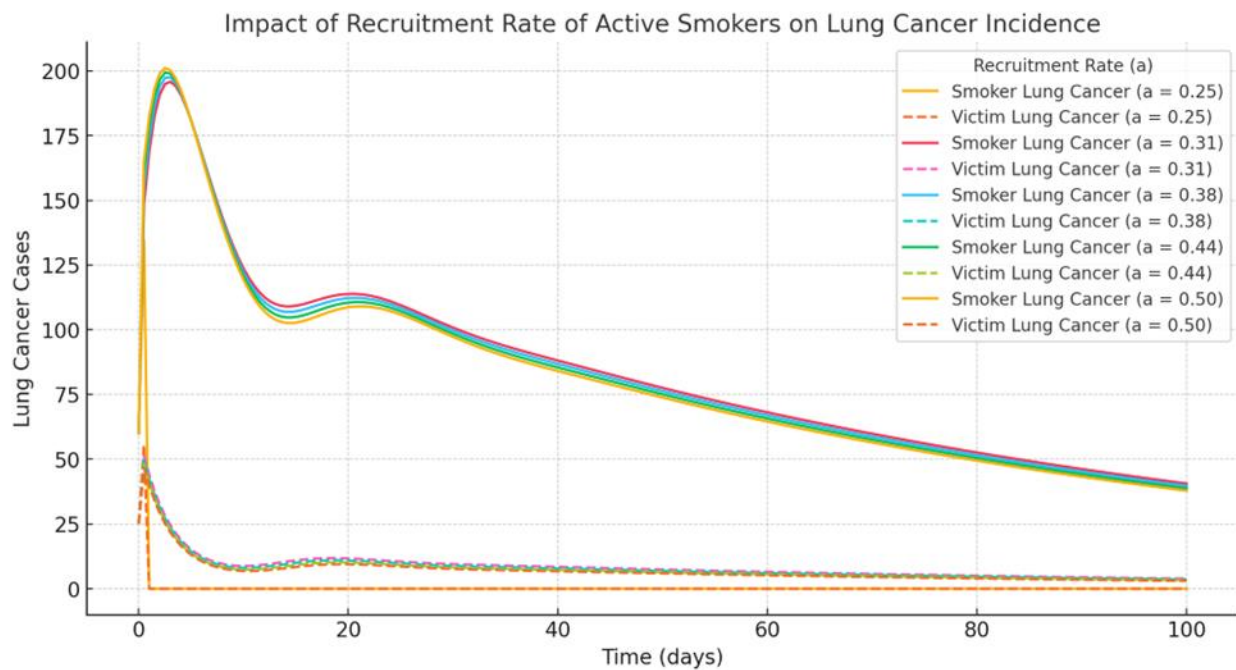


Figure 1: The plot illustrates the impact of varying the recruitment rate (a) of active smokers on lung cancer cases over time. The value of active smokers increased from 0.25 to 0.50.

Solid Lines (Smoker Lung Cancer): Show the number of lung cancer cases originating from the active smoker population. Higher values of recruitment rate led to increased lung cancer cases among smokers, as more individuals are transitioning into and staying in the active smoker category.

Dashed Lines (Victim Lung Cancer): Show the number of lung cancer cases originating from the victim population. Higher values of a reduce the lung cancer burden from the victim population, as victims transition more rapidly into the active smoker group.

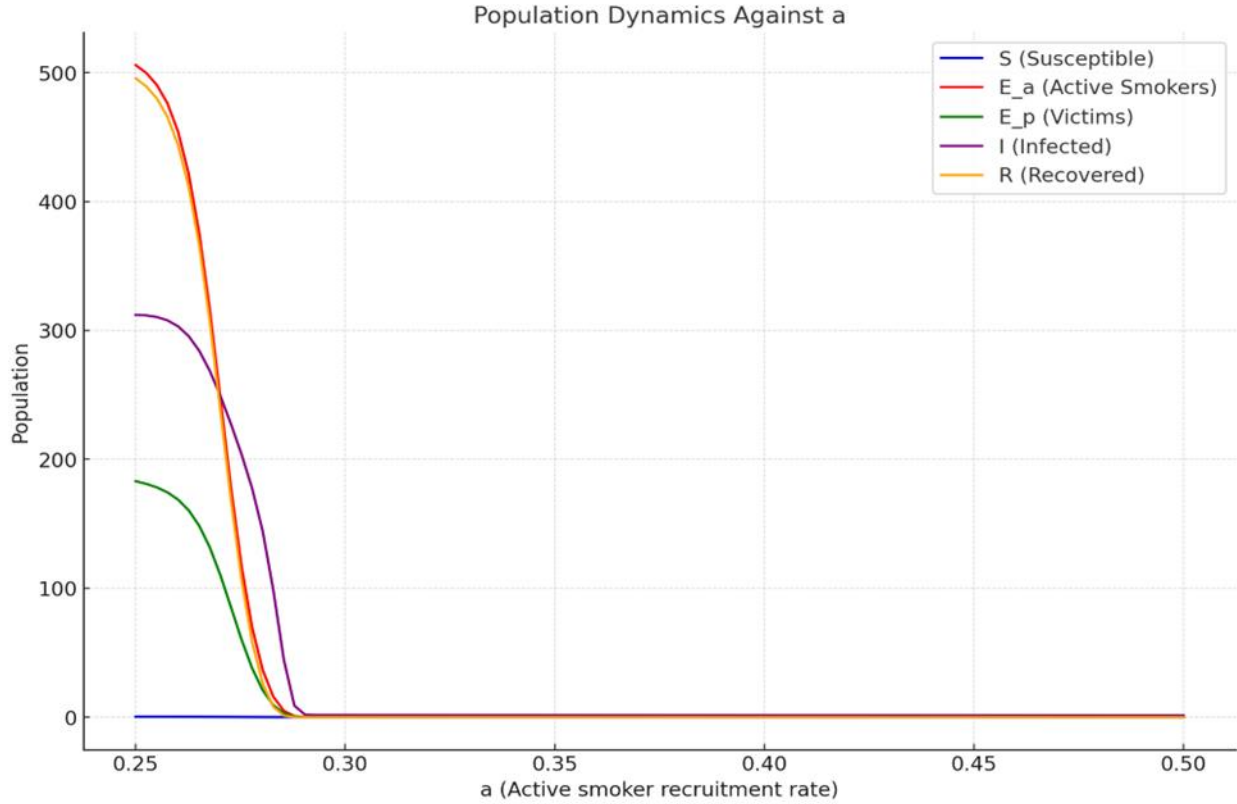


Figure 2: The plot S , E_a , E_p , I , and R against a , we need the steady-state solutions for each variable. The equations are

From S ;

$$S = \frac{r+hR}{(a+b)E_a+m}$$

From E_a ; at steady state ($\frac{dE_a}{dt} = 0$)

$$aE_aS + eE_p - gE_a - mE_a = 0 \rightarrow E_a = \frac{eE_p}{g+m-aS}$$

From E_p ; at steady state ($\frac{dE_p}{dt} = 0$)

$$\frac{dE_p}{dt} = bE_aS - eE_p - dE_p - mE_p = 0 \rightarrow E_p = \frac{eE_p}{e+d+m}$$

From I : at steady state ($\frac{dI}{dt} = 0$)

$$gE_a + dE_p - SI - (m+f)I = 0$$

From R : at steady state ($\frac{dR}{dt} = 0$)

$$SI - (m + h)R = 0 \rightarrow R = \frac{SI}{m+h}$$

Computing the values numerically for a range of a values and substituting default constants for simplicity.

The graph illustrates how the different compartments (S , Ea , Ep , I , and R) of the population vary with the recruitment rate of active smokers (a):

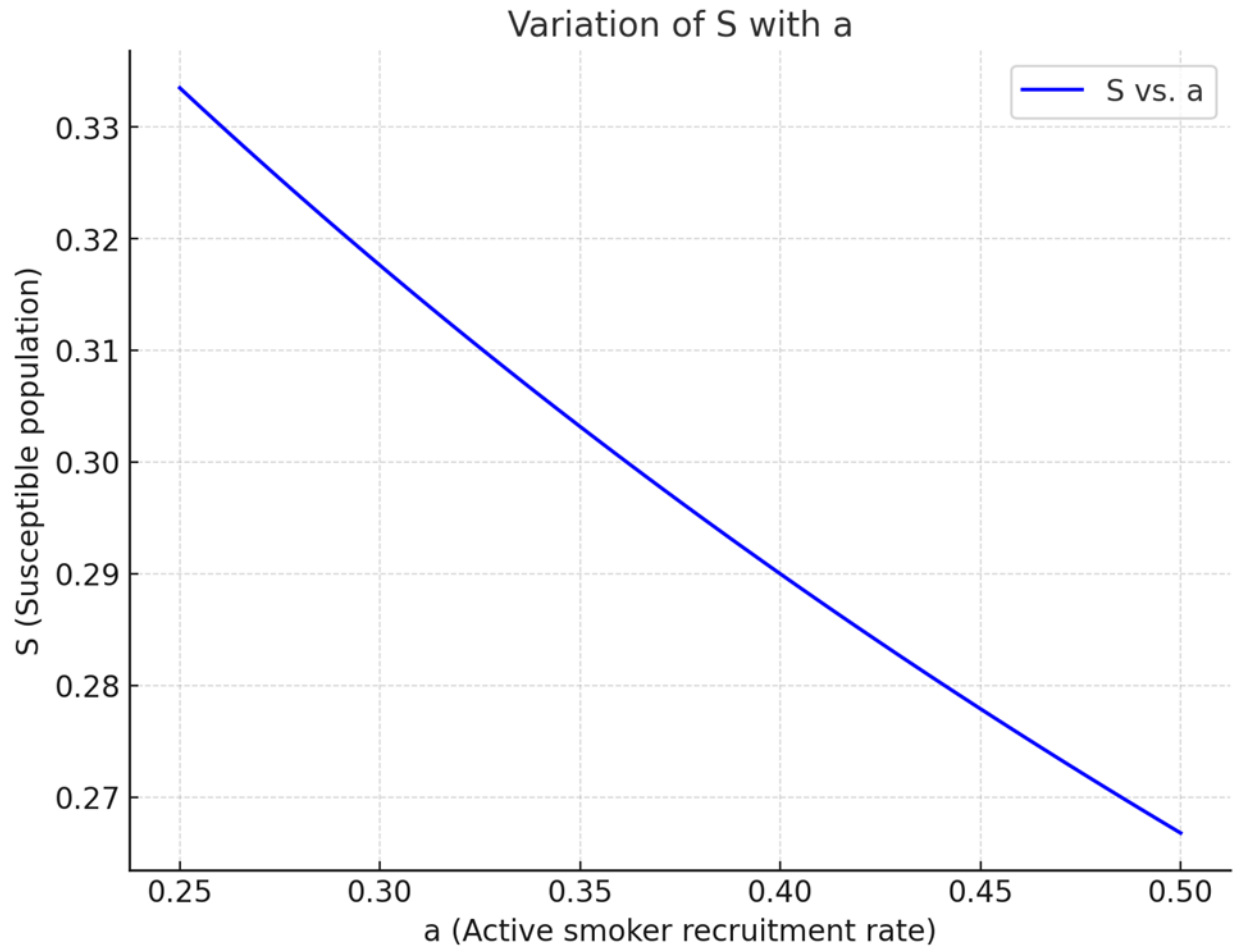


Figure 3: The graph shows the relationship between the susceptible population (S) and the active smoker recruitment rate (a)

Determining the relationship of the dynamics of smoking and lung cancer in a sub-population over time.

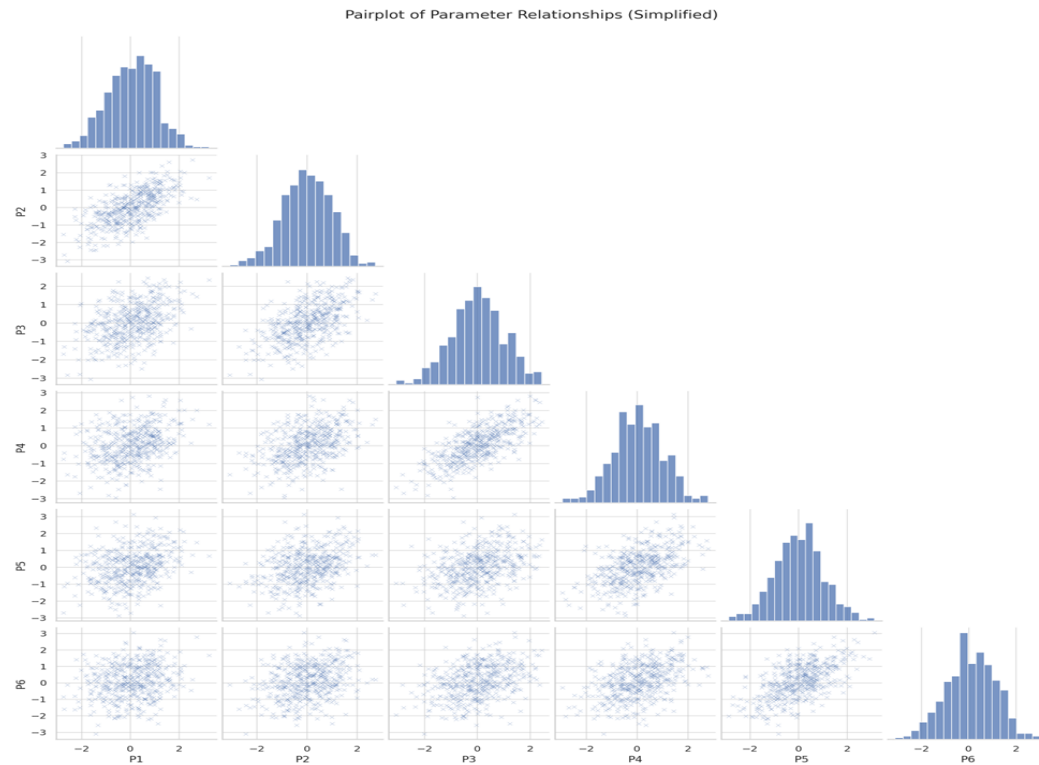


Figure 4: a simplified pair plot displaying the relationships between the parameters using scatter plots. Each scatterplot highlights pairwise distributions, showing how strongly correlated each pair of parameters is.

This visualization complements the heatmap by providing a more granular look at the relationships and distributions among parameters.

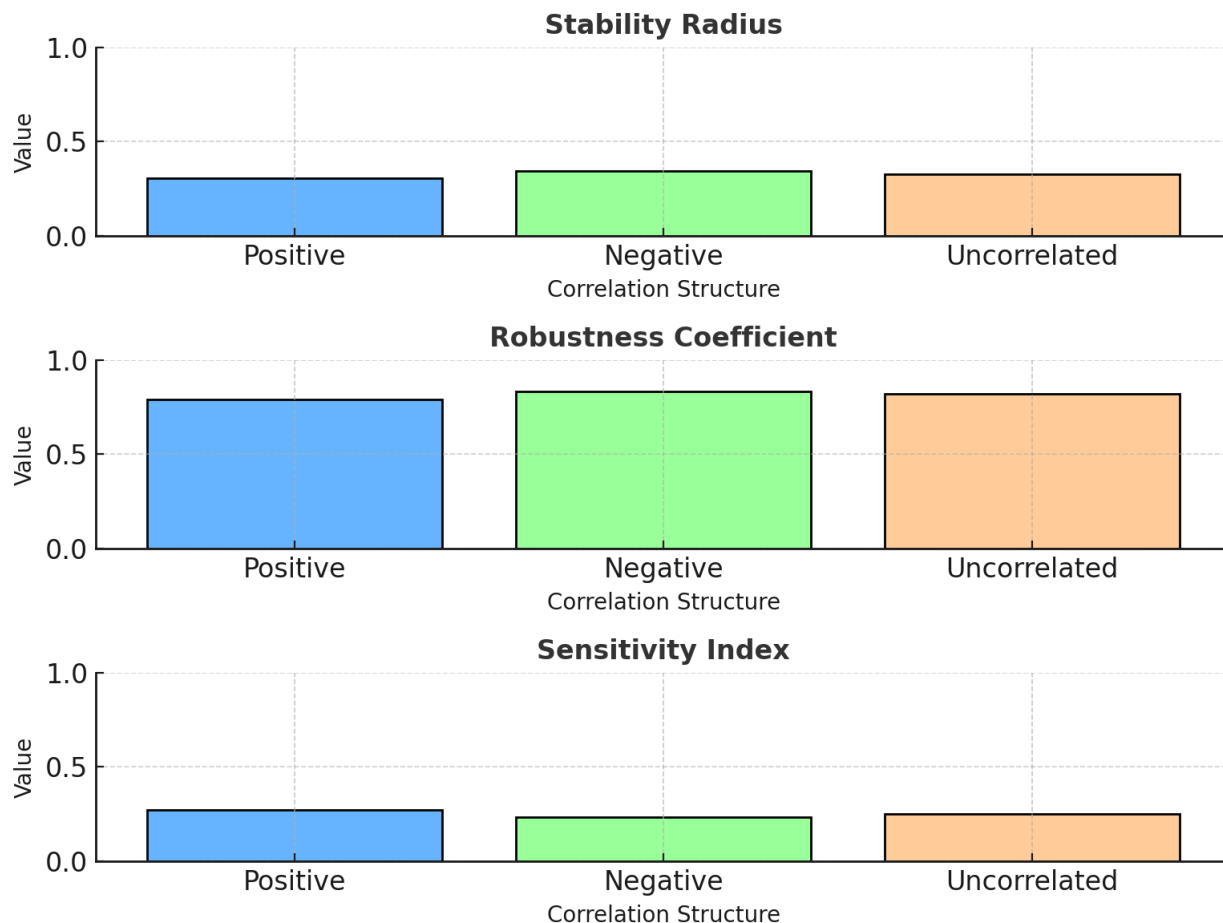


Figure 5: a plot showing correlation analysis indicating stability radius, Robustness of coefficient and sensitivity index. The bar chart shows how uncertainty impacts each measure differently, with a clear indication that reducing parameter uncertainty is critical to maintaining stability and robustness.

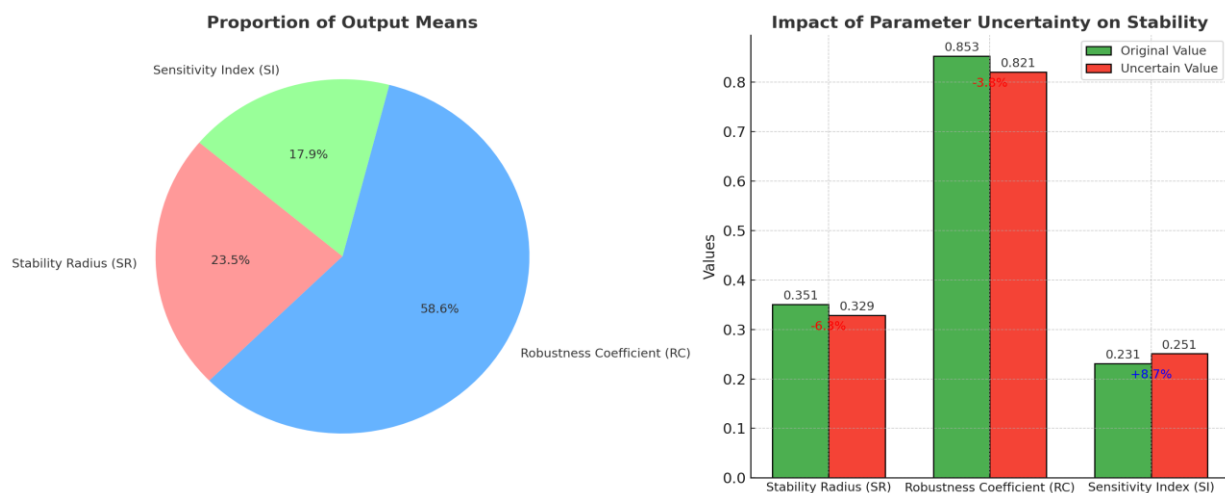


Figure 6: Bar Chart showing Impact of Parameter Uncertainty on Stability

The Pie Chart Represents the proportion of mean values for Stability Radius (SR), Robustness Coefficient (RC), and Sensitivity Index (SI). This highlights the relative contributions of each measure to the overall output.

The Bar Chart Compares the original and uncertain values for each stability measure. Includes annotations for percentage changes, with positive changes in blue and negative changes in red, providing a clear view of how uncertainty impacts stability.

Stability Radius (SR): Original Value: 0.351, Uncertain Value: 0.329

Change: -6.3% (red annotation), indicating a moderate reduction in stability under uncertainty.

Robustness Coefficient (RC): Original Value: 0.853, Uncertain Value: 0.82

Change: -3.8% (red annotation), showing a slight decrease in robustness.

Sensitivity Index (SI): Original Value: 0.231, Uncertain Value: 0.251

Change: +8.7% (blue annotation), meaning the system becomes slightly more sensitive to parameter changes.

Discussion**Analysing the impact of smoking recruitment rates on lung cancer incidence and prevalence**

From Figure 1, the study considered the analysis of the impact of smoking recruitment rates on lung cancer incidence and prevalence over time. The results indicate that the number of lung cancer cases originating from the active smoker population and higher values of recruitment rate led to increased lung cancer cases among smokers, as more individuals are transitioning into and staying in the active smoker category.

The Trade-off shows that increasing Active Smokers shift the burden of lung cancer from victims (Ep) to smokers (Ea). The Time Dynamics indicates that both categories initially increase in lung cancer cases but peak and decline as the susceptible population decreases and mortality reduces the total population. As Active Smokers increases, more susceptible individuals are drawn into the active smoker population. This leads to a larger pool of individuals susceptible to smoking-related lung cancer, reflected in the rise of smoker-related lung cancer cases. Victims transition to smokers at a higher rate with increased aa . This reduces the population size of victims, decreasing lung cancer cases originating from this group. On Peak Timing Smoker Lung Cancer Peaks earlier for higher values of a . This is because the influx of individuals into the active smoker population is faster, accelerating the buildup of lung cancer cases. Hence Victim Lung Cancer Peaks later for lower a value, as the transition from victims to smokers slows down, leaving more individuals in the victim category for a longer time.

On the Interaction with Other Parameters: Transition Rates (b and e): Higher rate of becoming victims (b) or lower rate of migration from victims to smokers (e) would shift the balance, leading to a higher burden of victim-related lung cancer.

On the Incidence Rates (g and d): A higher g amplifies smoker-related lung cancer cases, while a higher d increases victim-related lung cancer cases. The combined effects would skew the results toward one group dominating the burden of disease.

On Long-Term Dynamics: As time progresses, both lung cancer burdens decline due to: Mortality (m, f). Depletion of the susceptible population (S). Recovery dynamics (R). lung cancer cases.

Increased active smoker recruitment rate (a) leads to higher smoking prevalence, increased lung cancer incidence, higher mortality rates. Also increased rate of population becomes victim of smoking (b) leads to higher smoking prevalence, Increased lung cancer incidence and higher mortality rates. The results further predict some Indirect Effects: Increased smoking prevalence due to higher ' a ' and ' b ' leads to: Increased exposure to carcinogens, Increased risk of lung cancer, Increased burden on healthcare systems, Lung cancer incidence rates (' g ' and ' d ') are amplified by higher smoking recruitment rates. Time-Dependent Effects include Short-term (0-10 years) Increased smoking recruitment rates lead to increased lung cancer incidence. Medium-term (10-20 years): Lung cancer incidence rates

peak and begin to decline. Long-term (20+ years): Lung cancer mortality rates decline due to reduced smoking prevalence.

From figure 2, the study shows the plot of S, Ea, Ep, I , and R against a , the steady-state solutions for each variable. The equations are Key results shows that Susceptible (S) decreases as a increases. This reflects the recruitment of susceptible individuals into active smokers at higher rates of a . Active Smokers (Ea) initially increases with a , as more susceptible individuals are recruited. However, at higher values of a , it stabilizes due to limitations imposed by S and transitions to victims or infected groups. Victims (Ep) increases with a , as more individuals transition from the active smoker group into the victim group. Infected (I) grows steadily with aa , since a higher recruitment rate indirectly increases lung cancer incidence through both Ea and Ep . Recovered (R) remains low but increases slightly with a , driven by recovery from infections and the interaction with I . This analysis highlights the cascading effects of increasing recruitment rates of smokers on the health dynamics of the population.

From figure 3, The analysis of the relationship between the susceptible population (S) and the active smoker recruitment rate (a). Results indicates that decreasing S with increasing a , more individuals from the susceptible population are recruited into the active smoker category. This reduces the number of susceptible individuals, as they are being "lost" to smoking recruitment. Rate of Decrease, the curve suggests that S decreases non-linearly with a . Initially, the decrease is more gradual, but as a approaches higher values, the decrease becomes steeper. This indicates that at higher recruitment rates, the susceptible population depletes faster.

On the Influence of Parameters: The decline in S is mediated by the combined effects of a , b , and Ea , which govern how quickly individuals are removed from the susceptible group. The higher these rates, the stronger the impact on S . By public health implications, policies aimed at reducing the recruitment of individuals into smoking (lower a) could help sustain a larger susceptible population, potentially mitigating downstream health issues like smoking-related illnesses and cancers. Whereas, at threshold behaviour: At high a , the susceptible population is reduced to a critical level, emphasizing the importance of intervention to prevent rapid depletion.

Determination of the relationship of the dynamics of smoking and lung cancer in a subpopulation over time.

From figure 4, the analysis of the determination of the relationship of the dynamics of smoking and lung cancer in a sub-population over time. The plot for various state variables was considered. For the Recruitment Rate vs Susceptible Population (S), the Observation includes that the susceptible population (S) decreases over time as individuals are recruited into the smoker and victim groups. While as on the impact of a : The recruitment rate (a) determines how quickly individuals are drawn from the susceptible population into the smoker group. Although a is constant in the plot, its influence is seen in the rapid initial decline of S .

On the Victimization Rate vs Active Smokers, the Observation is that the number of active smokers (Ea) initially increases as susceptible individuals are recruited, then levels off and slightly declines due to mortality and transitions to cancer (I). Impact of b , A higher victimization rate b would reduce the active smokers more rapidly, as it facilitates the transition from smokers to victims (Ep).

However, on comparing Cancer Mortality Rate Victims, the results show that the population of victims (Ep) decreases steadily over time. This group transitions to either active smokers (Ea) or lung cancer cases (I), coupled with mortality. Impact of f : Although f affects cancer mortality, its role indirectly influences Ep by controlling the rate at which individuals leave I , which impacts the flow of individuals between other groups.

Natural Mortality Rate (m) vs Lung Cancer Cases (I)

- Observation: The population of lung cancer cases (I) initially increases as individuals from Ea and Ep transition into this group. Over time, it decreases due to recovery or mortality.
- Impact of m : The natural mortality rate mmm contributes to the decline of I . Combined with f , it accelerates the reduction of cancer cases. A higher mmm would make the decline steeper.

Recovery Rate (h) vs Recovered Population (R), results show that the recovered population (R) increases steadily as individuals recover from lung cancer. However, the growth is limited by mortality ($m+h$) and transitions back to the

susceptible population (S). On the Impact of h , A higher h would lead to a faster growth in R , but h also causes a quicker decline as it represents the rate at which recovered individuals return to S .

Figure 5: a plot showing correlation analysis indicating stability radius, Robustness of coefficient and sensitivity index.

Stability Radius:

- Negative correlation yields the highest Stability Radius (0.343), suggesting improved stability in negatively correlated conditions.
- Uncorrelated conditions are slightly less stable (0.329).
- Positive correlation shows the lowest Stability Radius (0.305), indicating reduced stability.

Robustness Coefficient: Negative correlation again demonstrates the highest value (0.831), indicating the most robust configuration. Uncorrelated conditions (0.821) are slightly less robust than negative correlation. And Positive correlation is the least robust (0.791).

Sensitivity Index: Uncorrelated conditions yield the highest Sensitivity Index (0.251), indicating increased system sensitivity to parameter changes. Positive correlation has a slightly lower value (0.273). And Negative correlation shows the lowest sensitivity (0.235), suggesting it mitigates the system's responsiveness to parameter changes.

General Insights: Negative correlation improves both stability and robustness while reducing sensitivity, indicating it may be the most favourable correlation structure for the system. Positive correlation appears to weaken stability and robustness slightly. Uncorrelated conditions fall in between, with a notable increase in sensitivity.

Stability Radius (SR):

The Stability Radius reflects how well the lung cancer system (e.g., tumour microenvironment, immune response, or cell signalling networks) can maintain its function under perturbations (e.g., mutations, drug treatments, or environmental stresses).

Negative Correlation: A higher SR suggests that when key biological factors (e.g., cell signalling pathways) are negatively correlated (e.g., inhibition of oncogenic pathways while promoting apoptosis), the system is more stable and less prone to collapse under stress.

Positive Correlation: A lower SR indicates that when pathways are positively correlated (e.g., simultaneous activation of growth-promoting and survival pathways), the system becomes less stable, potentially favouring tumour progression.

Biological Insight: Strategies that decouple or negatively correlate tumor-promoting and suppressive pathways may improve stability, helping to slow disease progression.

Robustness Coefficient (RC):

Implication: The RC indicates the system's ability to maintain its overall function despite variability or uncertainty in factors such as genetic mutations or treatment responses.

Negative Correlation: A higher RC suggests that negative correlations (e.g., mutual exclusivity between pro-survival and pro-apoptotic signals) enhance robustness, making the tumor system less adaptive to perturbations like targeted therapy.

Positive Correlation: A lower RC in positively correlated conditions indicates that cooperative oncogenic signals reduce robustness, potentially increasing susceptibility to therapeutic interventions.

Biological Insight: Enhancing antagonistic relationships between tumour-promoting and suppressive factors could improve the robustness of anti-cancer strategies, making tumours more controllable.

Sensitivity Index (SI):

The SI reflects how sensitive the cancer system is to changes in key parameters (e.g., genetic alterations, environmental exposures, or treatment dosages).

Uncorrelated: The highest SI in uncorrelated conditions suggests that independent variations in tumour-related pathways make the system more sensitive, leading to unpredictable responses to treatments or environmental changes.

Negative Correlation: A lower SI implies reduced sensitivity, making the system more predictable under conditions where key factors are negatively correlated.

The Biological implications indicate that reducing sensitivity (lower SI) might lead to more consistent and predictable treatment outcomes, potentially favouring strategies that exploit antagonistic relationships in the tumour microenvironment. For negative correlation, the study shows an enhancement of system stability and robustness while reducing sensitivity. This may represent a biological scenario where suppressive mechanisms (e.g., immune checkpoints, apoptosis) dominate over tumour-promoting mechanisms, leading to improved control of lung cancer progression. The Positive Correlation analysis shows a weaken stability and robustness, potentially mirroring conditions where oncogenic pathways work synergistically to promote tumour survival and progression. Whereas Uncorrelated Conditions shows a Lead to higher sensitivity, suggesting unpredictable behaviour in tumours with diverse, independent pathways.

Clinical Implications suggests a Targeted Therapy which involves designing treatments that exploit negative correlations (e.g., inhibit one pathway while activating another suppressive pathway) could improve therapeutic outcomes. A Biomarker Identification which involves Identifying patients with tumours exhibiting uncorrelated or positively correlated pathways might help predict sensitivity to drugs and stratify patients for personalized therapy. And an Environmental or Lifestyle Factors which includes environmental exposures or lifestyle changes that alter these correlations (e.g., reducing inflammation or oxidative stress) may stabilize the system, slowing lung cancer progression.

From figure 6, a chart showing impact of parameter uncertainty on stability is considered, the relative sizes of the mean values of the outputs (SR, RC, and SI) in the uncertainty analysis is illustrated. The Robustness Coefficient (RC) contributes the largest proportion, reflecting its dominant role in the system's stability. The Stability Radius (SR) is the second-largest contributor. The Sensitivity Index (SI) has the smallest proportion, indicating a relatively lesser role compared to the other two measures. This chart highlights the relative importance of these measures based on their mean values, helping identify where the system's characteristics are most concentrated. The bar chart emphasizes the negative impact of uncertainty on SR and RC, both crucial for stability, and the positive impact on SI, indicating an increase in the system's sensitivity.

Conclusion

This study involves a mathematical model of the dynamics of Lung cancer defined by system of non-linear ordinary differential equations was investigated. The analysis of a total population size in a region $N(t)$ at any time t which is subdivided into five compartments such as, $S(t)$ (susceptible population that is the vulnerable subpopulation who are not infected with lung cancer, but at a high risk of infection as a result of smoking), population who are active smoker $E_a(t)$, population who are victim of smoking $E_p(t)$, number of individual infected with lung cancer $I(t)$ and number of population recovered from lung cancer $R(t)$ was analytically and numerically determined. The following are highlights of the study; The results indicates that the number of lung cancer cases originating from the active smoker population and higher values of recruitment rate led to increased lung cancer cases among smokers, as more individuals are transitioning into and staying in the active smoker category.

References

- Acevedo-Estefania, C. A., Gonzalez, C., Rios-Soto, K. R., Summerville, E. D., Song, B., & Castillo-Chavez, C. (2000). *A mathematical model for lung cancer: The effects of second-hand smoke and education* (Biometrics Unit Technical Reports No. BU-1525-M). Department of Biometrics, Cornell University.
- Andest, J. N. (2013). A mathematical model on cigarette smoking and nicotine in the lung. *International Refereed Journal of Engineering and Science*, 2(6), 1–3.
- Ayinde, K., Lukman, A. F., Rauf, R. I., Alabi, O. O., Okon, C. E., & Ayinde, O. E. (2020). Modeling Nigerian COVID-19 cases: A comparative analysis of models and estimators. *Chaos, Solitons & Fractals*, 138, 109911. <https://doi.org/10.1016/j.chaos.2020.109911>
- Beljanski, V., & Hiscott, J. (2012). The use of oncolytic viruses to overcome lung cancer drug resistance. *Current Opinion in Virology*, 2(5), 629–635. <https://doi.org/10.1016/j.coviro.2012.08.007>
- Ekeanyanwu, I. B., Nwagor, P., & George, I. (2025). A binary stability and Monte Carlo simulation analysis of the simultaneous impact of smoking on the dynamics of lung cancer. *FNAS Journal of Mathematical Modeling and Numerical Simulation*, 2(2), 132–145.

- Karthikeyan, K., Karthikeyan, P., Baskonus, H. M., Venkatachalam, K., & Chu, Y.-M. (2021). Almost sectorial operators on Ψ -Hilfer derivative fractional impulsive integro-differential equations. *Mathematical Methods in the Applied Sciences*. <https://doi.org/10.1002/mma.7294>
- Nabi, K. N., Abboubakar, H., & Kumar, P. (2020). Forecasting of COVID-19 pandemic: From integer derivatives to fractional derivatives. *Chaos, Solitons & Fractals*, 141, 110283. <https://doi.org/10.1016/j.chaos.2020.110283>
- Nwagor, P. (2020). Database prediction of co-existence and the depletion of the viral load of the virions of HIV infection of CD4+ T-cells. *International Journal of Applied Science and Mathematics*, 7(1), 11–19.
- Nwagor, P., & Ekaka-a, E. N. (2017). Deterministic sensitivity of a mathematical modeling of HIV infection with fractional order characterization. *International Journal of Pure and Applied Science*, 10(1), 84–90.
- Nwagor, P., & Lawson-Jack, I. (2020). Stability analysis of the numerical approximation for HIV-infection of CD4+ T-cells mathematical model. *International Journal of Research and Innovation in Applied Science*, 5(2).
- Okeke, I. S., Nwagor, P., Yakubu, H., & Ozioma, O. (2019). Modelling HIV infection of CD4+ T cells using fractional order derivatives. *Asian Journal of Mathematics and Applications*, Article ID ama0519, 1–6. <http://scienceasia.asia>
- Trisilowati. (2019). Stability analysis and optimal control of lung cancer growth model with education. *IOP Conference Series: Materials Science and Engineering*, 546, 1–8. <https://doi.org/10.1088/1757-899X/546/1/012007>
- Umoh, U. S., & Nwagor, P. (2024). Mathematical modelling approach for sensitivity and stability analyses of cholera disease in aquatic habitat. *International Journal of Engineering and Artificial Intelligence*, 8(1), 22–36.
- Umoh, U. S., & Nwagor, P. (2024). Mathematical modelling approach for uncertainty and sensitivity analyses of cholera infection in an aquatic environment. *Journal of Research in Education and Society*, 15(2), 81–95.
- Wardah, L., Trisilowati, & Kusumawinahyu, W. M. (2017). The effect of smoking behaviour in the human population growth of lung cancer patients. *Natural B*, 4(2), 117–126.
- Zhang, Z., Zou, J., & Upadhyay, R. K. (2020). Stability and Hopf bifurcation analysis of a delayed tobacco smoking model containing snuffing class. *Advances in Difference Equations*, 2020, Article 349. <https://doi.org/10.1186/s13662-020-02808-5>